



Published in final edited form as:

*Nat Med.* 2009 March ; 15(3): 338–344. doi:10.1038/nm.1930.

## Sensitive *in vivo* imaging of T cells utilizing a membrane bound *Gaussia princeps* luciferase enzyme

Elmer B Santos<sup>1,3</sup>, Raymond Yeh<sup>2</sup>, James Lee<sup>2</sup>, Yan Nikhamin<sup>2</sup>, Blesida Punzalan<sup>1,3</sup>, Bleserene Punzalan<sup>1,3</sup>, Krista La Perle<sup>4</sup>, Steven M Larson<sup>1,3</sup>, Michel Sadelain<sup>2,5,6</sup>, and Renier J Brentjens<sup>2,6</sup>

<sup>1</sup> Department of Radiology, Memorial Sloan Kettering Cancer Center, 1275 York Avenue, New York, NY, USA 10021

<sup>2</sup> Department of Medicine, Memorial Sloan Kettering Cancer Center, 1275 York Avenue, New York, NY, USA 10021

<sup>3</sup> Molecular Pharmacology and Chemistry Program, Memorial Sloan Kettering Cancer Center, 1275 York Avenue, New York, NY, USA 10021

<sup>4</sup> Research Animal Resource Center, Memorial Sloan Kettering Cancer Center, 1275 York Avenue, New York, NY, USA 10021

<sup>5</sup> Gene Transfer and Somatic Cell Engineering Laboratory, Memorial Sloan Kettering Cancer Center, 1275 York Avenue, New York, NY, USA 10021

<sup>6</sup> Center for Cell Engineering, Memorial Sloan Kettering Cancer Center, 1275 York Avenue, New York, NY, USA 10021

### Abstract

We developed a novel approach to bioluminescent T cell imaging (BLI) using a membrane-anchored form of the *Gaussia* luciferase (GLuc) enzyme, termed extGLuc, which we could stably express in both mouse and human primary T cells. *In vitro*, extGLuc<sup>+</sup> cells emitted significantly higher bioluminescent signal when compared to cells expressing GLuc, *Renilla* luciferase (RLuc), and membrane-anchored RLuc (extRLuc). *In vivo*, mouse extGLuc<sup>+</sup> T cells exhibited higher bioluminescent signal when compared to GLuc<sup>+</sup> and RLuc<sup>+</sup> T cells. Application of this imaging approach to human T cells genetically modified to express tumor-specific chimeric antigen receptors (CARs) enabled us to demonstrate *in vivo* CAR-mediated T cell accumulation in tumor, T cell persistence over time, and concomitant imaging of T cells and tumor cells modified to express firefly luciferase (FFLuc). This sensitive imaging technology has application to many *in vivo* cell based studies in a wide array of mouse models.

---

Correspondence: brentjer@mskcc.org.

#### Author Contributions

E.B.S. contributed to the design of the experiments, supervised the experiments, and generated the manuscript figures, R.Y. contributed to the design of the experiments, J.L. helped conduct experiments for figure 5 and supplemental figures 1 and 2, Y.N. assisted in the conduct experiments from figures 1–3, B.P. and B.P. assisted in the conduct of the *in vivo* experiments, K.L.P. contributed to the conduct and interpretation of histologic analyses, S.M.L. contributed to the design of the experiments, M.S. contributed to the design of the experiments and review of the manuscript, R.J.B. supervised the project, contributed to the design of the experiments, and wrote the manuscript.

## INTRODUCTION

Bioluminescent imaging (BLI) of cells modified to express luciferase enzymes allows for non-invasive monitoring of cells following adoptive transfer into mice. Firefly luciferase (FFLuc), derived from the firefly *Photinus pyralis*, which catalyzes the substrate luciferin<sup>1</sup>, is the most extensively utilized luciferase enzyme in cell-based BLI. While effective in monitoring immortalized cells *in vivo*<sup>2-4</sup>, the application of FFLuc to T cell imaging has been largely restricted to the study of T cell populations derived from transgenic FFLuc<sup>+</sup> mice, T cell hybridomas, and highly selected clonal FFLuc-transfected human T cells<sup>5-11</sup>. Furthermore, signal in T cells is markedly lower when compared to other FFLuc<sup>+</sup> hematopoietic cells or tumor cells<sup>6,11</sup>, and efforts by investigators to introduce the FFLuc gene into primary T cells have been compromised by poor gene expression<sup>12</sup>.

*Renilla* luciferase (RLuc), derived from the anthozoan sea pansy *Renilla reniformis*, catalyzes coelenterazine, a substrate distinct from luciferase<sup>1</sup>. While readily expressed by primary T cells, the use of RLuc in T cell BLI is compromised by low signal intensity impairing imaging of cells in deeper tissues thereby restricting imaging of T cell trafficking to superficial tumors<sup>13</sup>. The humanized *Gaussia* luciferase (GLuc) enzyme, derived from the copepod *Gaussia princeps*, likewise utilizes coelenterazine as a substrate but emits a markedly more intense signal and may therefore overcome limitations associated with RLuc<sup>14</sup>. However, the native GLuc enzyme is secreted<sup>14</sup> significantly attenuating the *in vivo* bioluminescent signal.

In this report, we show that this limitation may be overcome by genetically engineering GLuc through the addition of a CD8 transmembrane domain to the C-terminus of the enzyme allowing for retention of the resulting luciferase construct, extGLuc, to the cell surface. We show that extGLuc<sup>+</sup> T cells are rapidly generated from both mouse and human primary T cells and have a markedly superior *in vivo* bioluminescent signal when compared to GLuc<sup>+</sup> and RLuc<sup>+</sup> T cells. We further utilize this technology to demonstrate dual imaging of extGLuc<sup>+</sup> T cell and targeted FFLuc<sup>+</sup> tumor cell populations within the same mouse.

## RESULTS

### *In vitro* comparison of extGLuc to Gluc and RLuc

We transduced SFG retroviral constructs<sup>15</sup> containing the GLuc, extGLuc, RLuc, extRLuc, and GFP-FFLuc genes (Fig. 1a) into retroviral producing fibroblast cells (PG-13). Cultured GLuc<sup>+</sup> and extGLuc<sup>+</sup> fibroblasts emitted a significantly enhanced bioluminescent signal when compared to RLuc<sup>+</sup> and extRLuc<sup>+</sup> fibroblasts (Fig. 1b,c). Following subtraction of signal present in the media, extGLuc<sup>+</sup> fibroblasts emitted a 100 fold greater signal when compared to fibroblasts expressing either RLuc or extRLuc, and a >9 fold increased signal when compared to GLuc<sup>+</sup> fibroblasts (Fig. 1c).

Fibroblasts expressing extGLuc and GLuc demonstrated a plateau signal of 10 minutes representing a >10 fold increased signal when compared to fibroblasts expressing RLuc (Fig. 1d). We further verified surface expression of the extGLuc construct in human T cells retrovirally transduced to express extGLucIRES-GFP, GLucIRES-GFP, or extGLuc by FACS (Fig. 1e) and immunohistochemical analyses (Fig. 1f).

### Enhanced signaling by extGLuc<sup>+</sup> T cells *in vivo*

We compared *in vivo* bioluminescent signal from C57BL6 primary T cells transduced to express extGLuc, RLuc, or GLuc, following intravenous injection into MHC-mismatched SCID-Beige mice generating *in vivo* T cell expansion as a result of graft versus host disease. All T cell groups had similar gene transfer, and infused T cells were normalized to the GFP<sup>+</sup> fraction. Comparison to T cells transduced with the SFG GFP-FFLuc construct was not

performed due to poor gene transfer efficiencies (<3%) (data not shown). We found a statistically significant greater bioluminescent signal (six to 17 fold) in mice infused with extGLuc<sup>+</sup> T cells when compared to mice infused with either RLuc<sup>+</sup> or GLuc<sup>+</sup> T cells (Fig. 2a,b).

While we noted a signal decay in the extGLuc<sup>+</sup> T cell infused mice over time (Fig. 2c), >50% of signal was retained at 4 min following bolus intravenous injection of coelenterazine (Fig. 2d). We further demonstrated presence of extGLuc<sup>+</sup> T cells in tissues typically involved with BLI (Fig. 2e) and histologic analyses (Fig. 2f) at autopsy.

### ***In vivo* trafficking of extGLuc<sup>+</sup> DO11.10 OVA-specific T cells**

We injected SCID-Beige mice subcutaneously with A20 mouse lymphoma tumor cells expressing OVA (A20(OVA)) in the right flank, and as a control, A20 tumor cells expressing GFP (A20(GFP)) in the left flank, and at d 7 mice injected mice intravenously with extGLuc<sup>+</sup> OVA-specific DO11.10 transgenic T cells. BLI demonstrated initial T cell localization to the lungs which decreased over time with progressively increasing signal in the A20(OVA) tumor consistent with either migration of T cells to the OVA<sup>+</sup> tumor, or proliferation of T cells within the tumor (Fig. 3a). We assessed tumor size by positron emission tomography (PET) prior to and at d 13 following T cell infusion (Fig. 3b) demonstrating stable FDG signal in the targeted A20(OVA) tumor consistent with anti-tumor activity of DO11.10 T cells, in contrast to progressive signal observed in the A20(GFP) tumor (Fig. 3c). We confirmed the presence of DO11.10 T cells in the A20(OVA) but not A20(GFP) control tumor by immunohistochemistry at autopsy (Fig. 3d).

In order to demonstrate the utility of T cell imaging with extGLuc in the context of a competent immune system, we injected Balb/c mice with wild-type A20 tumor (left flank) or A20(OVA) tumor (right flank) followed at d 7 with infusion of extGLuc<sup>+</sup> DO11.10 T cells. Once again, we noted specific T cell signal in the A20(OVA), but not the wild type A20 tumor (Fig. 3e).

### ***In vivo* monitoring of tumor-targeted extGLuc<sup>+</sup> human T cells**

Human T cells genetically modified to express a CD19 targeted chimeric antigen receptor (CAR), 19z1, can eradicate human systemic CD19<sup>+</sup> Raji Burkitt lymphoma tumors, which primarily localize to the bone marrow in SCID-Beige mice<sup>16</sup>. SCID-Beige mice bearing human systemic CD19<sup>+</sup> acute lymphoblastic leukemia (NALM-6) tumors, which infiltrate the bone marrow, liver, spleen, lymphnodes, lungs, and CNS, are more difficult to fully eradicate following infusion with T cells expressing either the first generation 19z1 CAR<sup>16</sup> or the second generation 1928z CAR which has additional CD28-mediated co-stimulatory activity<sup>17</sup>.

To determine whether treatment failure in the NALM-6 tumor model was related to a defect in T cell accumulation at selected sites of systemic tumor, we initially assessed whether human T cells, co-transduced to express both the 19z1 CAR and extGLuc, specifically accumulate in subcutaneous NALM-6 tumors in SCID-Beige mice (Fig. 4a). T cells co-transduced with the Pz1 CAR<sup>18</sup> and extGLuc, served as a control. Following T cell injection, only mice treated with 19z1<sup>+</sup>extGLuc<sup>+</sup> T cells displayed signal in the tumor (Fig. 4a). We verified the presence of human T cells in the tumor of 19z1<sup>+</sup>extGLuc<sup>+</sup> but not Pz1<sup>+</sup>extGLuc<sup>+</sup> T cell treated mice by immunohistochemistry (Fig. 4b).

We next generated a bicistronic SFG construct containing the second generation 1928z CAR, previously demonstrated to have superior *in vivo* anti-tumor efficacy against the NALM-6 tumor cell line<sup>17</sup>, and extGLuc (1928zIRES-extGLuc) (Fig. 5a). T cells transduced with Pz1IRES-extGLuc served as a control. Expression of extGLuc on the T cell surface did not impair CAR-mediated T cell function by a standard 4 hour <sup>51</sup>Cr release cytotoxicity assay (Fig.

5b), expansion studies following co-culture on NIH-3T3 fibroblasts expressing CD19 and CD80<sup>16,17</sup>, and cytokine release profiles measuring IL-2 and IFN- $\gamma$  which demonstrated similar results between activated 1928zIRES-extGLuc<sup>+</sup> and 1928z<sup>+</sup> T cells (data not shown).

We injected SCID-Beige mice systemically with GFP-FFLuc<sup>+</sup> NALM-6 tumor on d-10, and monitored tumor burden by BLI ten days later (d 0). T cell imaging in 1928zIRES-extGLuc<sup>+</sup> T cell treated mice, in contrast to control mice treated with Pz1IRES-extGLuc<sup>+</sup> T cells, demonstrated signal coincident with FFLuc signal from NALM-6 tumor seen on d 0, on d 1 and d 3 consistent with specific accumulation, activation, and possible proliferation of CD19-targeted T cells at systemic sites of tumor involvement. (Fig. 5c). 1928zIRES-extGLuc<sup>+</sup> T cell signal persisted over 7 days, and thereafter diminished with residual signal noted in the abdomen. Re-imaging of NALM-6 tumor with luciferase at d 11 following T cell infusion demonstrated isolated, persistent disease in the periodontal region in 2 of 6 mice (Fig. 5c), a site which significantly had no detectable bioluminescent T cell signal. The remaining mice demonstrated residual disease isolated solely in the bone marrow ( $n = 1$ ), spleen ( $n = 1$ ), moderate disease at multiple anatomical sites ( $n = 1$ ), or no detectable disease ( $n = 1$ ) (data not shown). As expected, control mice at d 11 demonstrated diffuse FFLuc bioluminescent signal consistent with tumor progression.

We sacrificed several treated mice on d 4 following T cell infusion for immunohistochemical analysis. At this time point, in 1928zIRES-extGLuc<sup>+</sup> T cell treated mice, in contrast to Pz1IRES-extGLuc<sup>+</sup> T cell treated mice, CD3<sup>+</sup> T cells were abundantly present at all anatomical sites with extGLuc bioluminescent signal, including the bone marrow (Fig. 5d), spleen, and liver (data not shown). Consistent with the anti-tumor efficacy of the CD19-targeted T cells, scant FFLuc<sup>+</sup> tumor was evident in the bone marrow (Fig. 5d), spleen and liver (data not shown) of treated mice, in contrast to abundant FFLuc<sup>+</sup> tumor present at all sites of control mice (Fig. 5d, and data not shown). At d 11, following tumor cell imaging, we sacrificed the remaining mice and analyzed tissues by immunohistochemistry. We detected persistent T cells in the liver of 1928zIRES-extGLuc<sup>+</sup> T cell treated mice, consistent with the extGLuc signal noted in the abdomen on d 7 and d 10 (Fig. 5d). We identified abundant tumor but no T cells in the liver of Pz1IRES-extGLuc<sup>+</sup> T cell treated mice (Fig. 5d). These data directly demonstrate, for the first time, that tumor-targeted CARs specifically mediate accumulation of T cells to systemic tumor *in vivo*.

To assess human T cell trafficking at early time points, we infused tumor free mice with extGLuc<sup>+</sup> T cells demonstrating brief isolated T cell signal only in the lungs at 15 and 60 min following T cell infusion (Supplemental Figure 1a online), a finding confirmed by FACS analysis (Supplemental Figure 1b online). No signal was noted elsewhere over 48 h in these studies, including mouse secondary lymphoid tissues (Supplemental Figure 2 online).

## DISCUSSION

Outside of the setting of transgenic FFLuc<sup>+</sup> mice wherein the study of FFLuc<sup>+</sup> T cells is restricted to specific mouse strains<sup>5,6</sup>, reports of BLI utilizing FFLuc<sup>+</sup> T cells are largely limited to studies requiring prior FACS sorting of GFP-FFLuc<sup>+</sup> murine primary T cells<sup>19</sup>, or cloned FFLuc<sup>+</sup> transduced human T cells<sup>11</sup>. Significantly, both approaches require lengthy *in vitro* culture conditions which may adversely affect T cell phenotype thereby limiting the relevance of subsequent *in vivo* studies<sup>20-22</sup>.

In order to image primary T cells at high sensitivity, as well as allow for dual T cell-FFLuc<sup>+</sup> tumor cell imaging, we studied the feasibility of using GLuc for T cell BLI. T cells expressing GLuc enzyme are rapidly generated by efficient retroviral transduction and expansion of both mouse and human primary T cells. GLuc emits a markedly enhanced signal intensity when

compared to RLuc and has been employed in cellular secretion assays, protein-protein interaction assays, and in *in vivo* antibody directed BLI imaging of tumor<sup>23–27</sup>. However, GLuc is secreted by the cell and previously published studies have demonstrated that genetic modification of GLuc to restrict secretion, either through the deletion of the signal peptide, or through the addition of a KDEL retention sequence, failed to enhance the cellular bioluminescent signal<sup>14</sup>.

Since GLuc generates a bioluminescent signal in an ATP-independent manner, we could harness this signal by anchoring the GLuc enzyme to the cell surface, an approach which may further overcome dampening of coelenterazine-based bioluminescent signals associated with *MDR1* P-glycoprotein mediated efflux of the substrate<sup>28</sup>. We found that T cells transduced with the resulting extGLuc enzyme could be rapidly generated *ex vivo* maintaining a favorable central memory phenotype, and allowed for sensitive *in vivo* detection even in deep tissues although the blue-green emission characteristics of the extGLuc construct may ultimately limit the sensitivity of detection in deeper tissues at lower T cell concentrations.

Because the FFLuc luciferin and GLuc coelenterazine substrates do not cross react, we can further concomitantly image FFLuc<sup>+</sup> tumor and extGLuc<sup>+</sup> T cells within the same mouse. Significantly, we were able to utilize this dual cell imaging technology to demonstrate CAR-mediated specific T cell accumulation to most sites of systemic tumor involvement, and that the unique, but likely clinically irrelevant, persistence of tumor in the periodontal area, seen in our tumor model as well as in others<sup>17,29</sup>, was a result of failed T cell entry or accumulation to this site, a hypothesis we postulated in a previous publication<sup>17</sup>.

Finally, in contrast to alternative approaches of *in vivo* T cell imaging including PET<sup>30</sup> and magnetic resonance imaging<sup>31–33</sup>, BLI as an imaging modality is readily accessible, financially feasible, allows for retained sensitivity over time with minimal background signal, and is amenable to concomitant imaging of 2 distinct cell populations. We conclude that the novel technology presented here represents a potent and readily utilized advance in the imaging of primary T cells.

## METHODS

### Generation of luciferase retroviral constructs

We subcloned GFP-FFLuc (Clontech Laboratories), humanized GLuc (Nanolight Technology), and RLuc (Promega Corporation) genes into the SFG retroviral vector<sup>15</sup>. To generate the extGLuc construct, we replaced the GLuc native signal peptide with residues 1–18 of the human CD8 leader peptide and removed the 3' GLuc stop codon by PCR. We fused the CD8 transmembrane domain corresponding to AA 137–212 with an additional stop codon at the 3' end to the resulting PCR product by overlapping PCR. We generated the extRLuc construct in a similar manner. We inserted an IRES-extGLuc cassette, generated by overlapping PCR, distal to the CAR gene to construct 1928zIRES-extGLuc and Pz1IRES-extGLuc.

### Retroviral gene transduction

We transfected Phoenix-Eco cells with SFG plasmid DNA using ProFection<sup>®</sup> Mammalian Transfection Systems (Promega Corporation). We generated modified T cells from mouse splenocytes following red blood cell lysis using ACK lysing buffer (Bio Whittaker), passage through nylon wool columns (Polysciences), activation with Mouse CD3/CD28 T cell Expander magnetic beads (Invitrogen Dynal) and transduction using Phoenix-Eco retroviral supernatants<sup>16,34</sup>. We generated PG-13 retroviral producer cell lines as described<sup>35</sup>.

We performed retroviral transduction of healthy human donor T cells, obtained following informed consent under the MSKCC institutional review board approved protocol #90-095, using PG-13 retroviral supernatants<sup>34</sup>, and subsequently expanded transduced T cells by co-culture on AAPCs<sup>16</sup>.

### Flow cytometry

FACs was performed using a FACScan cytometer with Cellquest software (BD Biosciences), utilizing a GLuc specific mouse monoclonal antibody (Nanolight Technology) followed by PE conjugated goat sera specific to mouse IgG (Caltag Laboratories), or PE labeled CAR specific monoclonal antibody 12D11 (MSKCC monoclonal antibody core facility). Cell suspensions obtained from mouse tissues were blocked using BD CD16/CD32 Mouse Fc Block (BD Pharmingen) prior to staining with human CD3 specific antibody (Caltag).

### *In vivo* mouse models

*In vivo* studies utilized 8 to 12 week old FOX CHASE C.B-17 (SCID-Beige), C57BL6, DO11.10, and Balb/c mice (Taconic, Germantown, NY). In GvHD studies, we injected  $5 \times 10^6$  extGLuc<sup>+</sup>GFP<sup>+</sup> C57BL6 derived T cells by tail vein into SCID-Beige or Balb/c mice. All A20 tumors were generated by subcutaneous injection of  $1 \times 10^6$  A20 tumor cells and treated with  $5 \times 10^6$  GFP<sup>+</sup> extGLuc<sup>+</sup> DO11.10 OVA specific transgenic T cells. SCID-Beige mice were injected with  $5 \times 10^7$  NALM-6 tumor cells to generate subcutaneous tumors, followed at d 14 by systemic infusion of  $1 \times 10^7$  transduced T cells. For systemic NALM-6(GFP-FFLuc) tumor studies, SCID-Beige mice were systemically injected with  $1 \times 10^6$  tumor cells followed at d 10 by  $1 \times 10^7$  transduced T cells. All murine studies were performed in the context of an MSKCC institutional animal care and use committee approved protocol (#00-05-065).

### Bioluminescence imaging

Bioluminescence was detected using a Xenogen IVIS Imaging System (Xenogen) as previously described<sup>36</sup>. We performed imaging either 10–15 sec following bolus IV injection with coelenterazine (250  $\mu$ g) (Nanolight Technology) or 10–15 min after intraperitoneal injection of D-luciferin (150 mg kg<sup>-1</sup>) (Xenogen). We imaged mice individually whenever coelenterazine substrate was used whereas 2–5 mice were simultaneously imaged in luciferin-based acquisitions. Time of image acquisition was in the range of 0.5 to 3 min. Field of view of 15, 20, or 25 cm with low, medium, or high binning in an open filter was utilized to maximize signal intensity and sensitivity. We performed *in vitro* bioluminescence imaging using similar acquisition parameters. We obtained acquisition of image data sets and measurement of signal intensity through region of interest (ROI) analysis using Living Image software (Xenogen), and normalized images displayed on each data set according to color intensity.

### MicroPET imaging

We imaged mice using a R4 microPET<sup>TM</sup> scanner (Concorde Microsystems) with 2-[<sup>18</sup>F]-fluoro-2 deoxy-D-glucose (<sup>18</sup>FDG) as described elsewhere<sup>16</sup>.

### Cytotoxicity assays

We assessed cytotoxicity of 1928zIRES-extGLuc, 1928z, Pz1IRES-extGLuc, and Pz1 transduced T cells by standard 4 h <sup>51</sup>Cr release assays as described elsewhere<sup>16,18</sup>.

### Cytokine detection

T cell cytokine secretion assays were conducted using the Luminex IS100 system with IS 2.3 software (Luminex Corp.)<sup>17</sup>.

## Histology

Hematoxylin and eosin (H&E) staining has been described elsewhere<sup>17</sup>. We probed fresh tissue samples embedded in optimal cutting temperature compound (Sigma-Aldrich) with biotinylated mouse antibody specific to human CD8 or mouse antibody specific to the DO11.10 TCR (Caltag Laboratories), cytospin preparations were probed with mouse antibody specific to GLuc followed by horse sera specific to mouse IgG. We detected antibody using the ARK Peroxidase Kit (DakoCytomation). After unmasking of epitopes with citrate buffer (10mM, microwave at high power for 15 min), we detected T cells and tumor cells in paraffin-embedded mouse tissues using rabbit polyclonal sera specific to human CD3 (DakoCytomation) and rabbit polyclonal sera specific to FFLuc (MBL International) followed by secondary antibody application (biotinylated goat sera specific to rabbit IgG) using the Vectastain ABC Elite Kit System (Vector Laboratories).

## Statistics

We determined statistical significance of data using analysis of variance (ANOVA) with SPSS software (SPSS Incorporated, Chicago, IL).

## Supplementary Material

Refer to Web version on PubMed Central for supplementary material.

## Acknowledgments

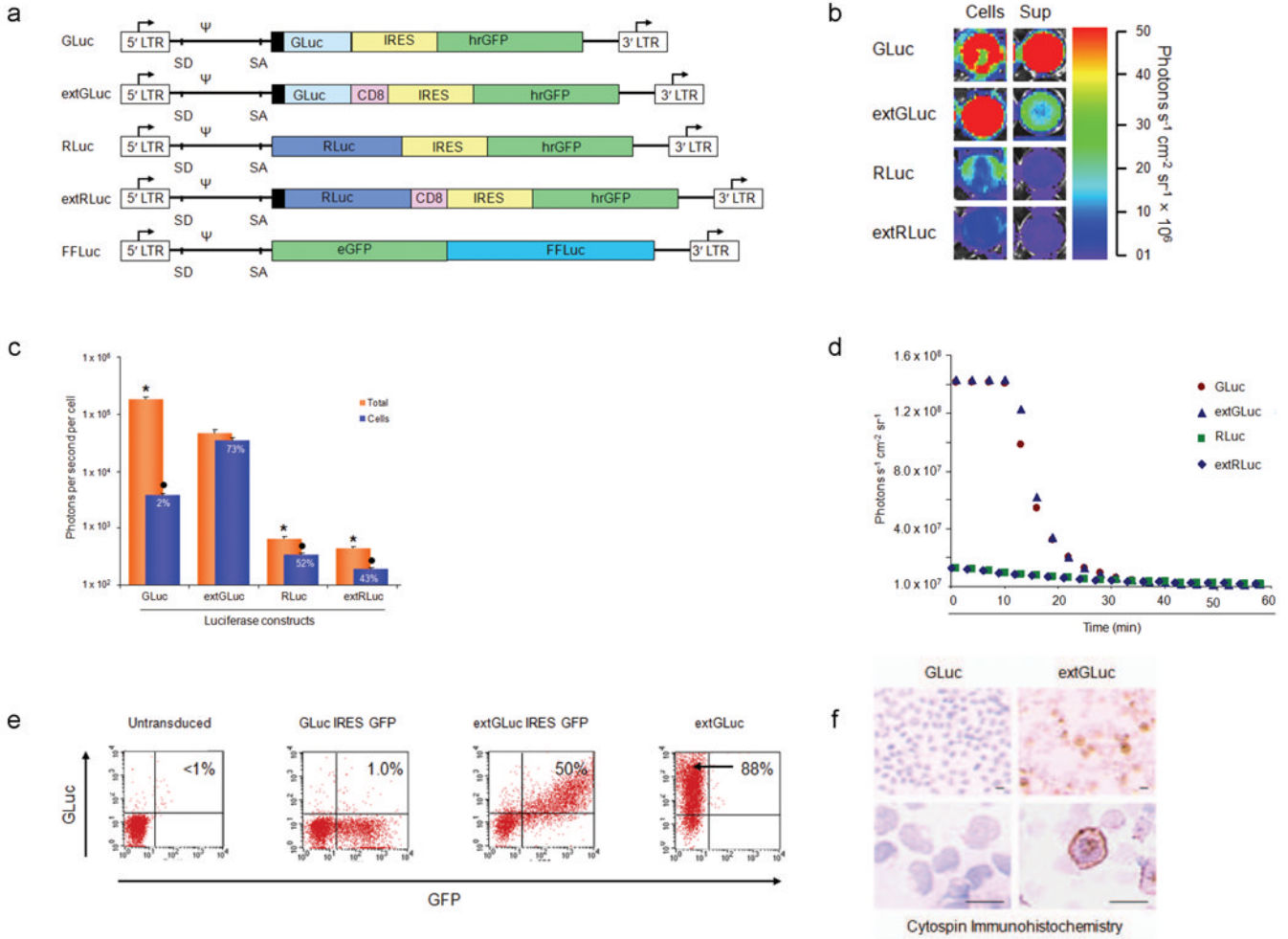
Supported by CA95152, CA059350, CA08748, CA86438, CA096945, CA094060, The Alliance for Cancer Gene Therapy, Damon Runyon Clinical Investigator Award (RJB), The Annual Terry Fox Run for Cancer Research (New York, NY) organized by the Canada Club of New York, Kate's Team, Mr. William H. Goodwin and Mrs. Alice Goodwin and the Commonwealth Cancer Foundation for Research and the Experimental Therapeutics Center of MSKCC, the Geoffrey Beene Cancer Foundation, the CLL Foundation, and the Bocina Cancer Research Fund.

## References

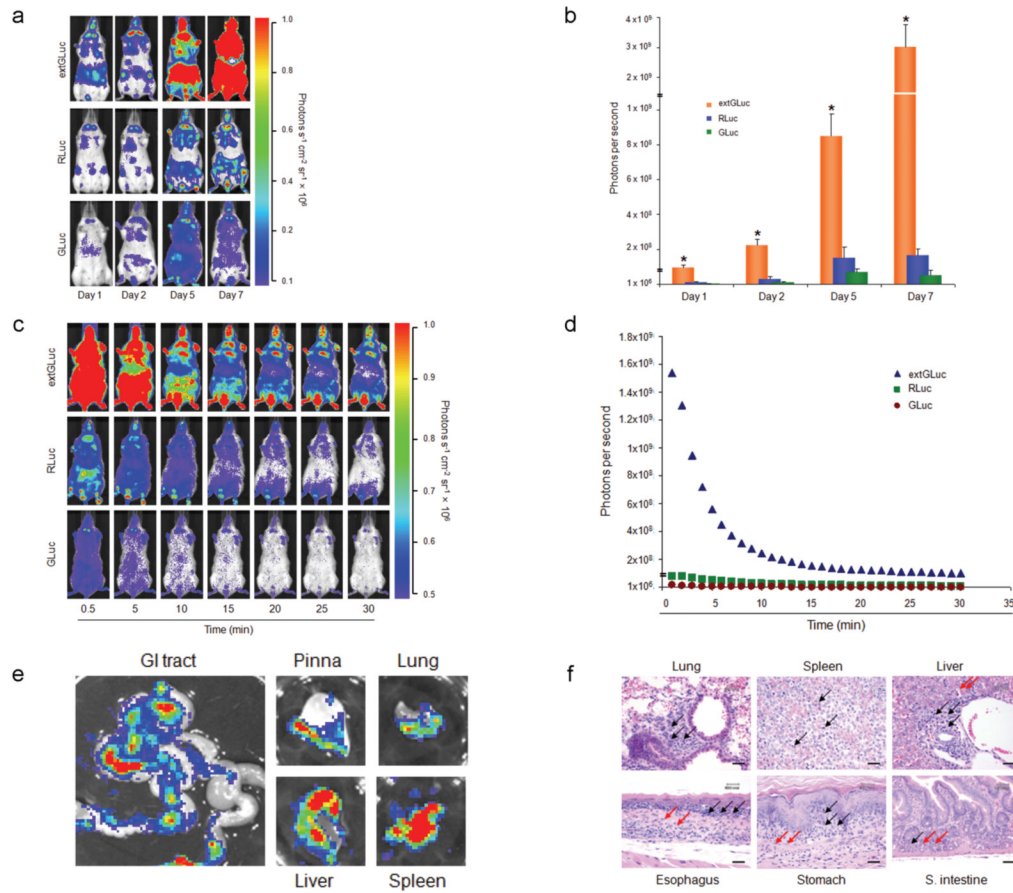
1. Greer LF 3rd, Szalay AA. Imaging of light emission from the expression of luciferases in living cells and organisms: a review. *Luminescence* 2002;17:43–74. [PubMed: 11816060]
2. Scheffold C, Kornacker M, Scheffold YC, Contag CH, Negrin RS. Visualization of effective tumor targeting by CD8+ natural killer T cells redirected with bispecific antibody F(ab')(2)HER2xCD3. *Cancer Res* 2002;62:5785–91. [PubMed: 12384539]
3. Edinger M, et al. Revealing lymphoma growth and the efficacy of immune cell therapies using in vivo bioluminescence imaging. *Blood* 2003;101:640–8. Epub 2002 Sep 26. [PubMed: 12393519]
4. Thorne SH, Negrin RS, Contag CH. Synergistic antitumor effects of immune cell-viral biotherapy. *Science* 2006;311:1780–4. [PubMed: 16556847]
5. Cao YA, et al. Shifting foci of hematopoiesis during reconstitution from single stem cells. *Proc Natl Acad Sci U S A* 2004;101:221–6. Epub 2003 Dec 19. [PubMed: 14688412]
6. Cao YA, et al. Molecular imaging using labeled donor tissues reveals patterns of engraftment, rejection, and survival in transplantation. *Transplantation* 2005;80:134–9. [PubMed: 16003245]
7. Beilhack A, et al. In vivo analyses of early events in acute graft-versus-host disease reveal sequential infiltration of T-cell subsets. *Blood* 2005;106:1113–22. Epub 2005 Apr 26. [PubMed: 15855275]
8. Zeiser RS, et al. Inhibition of CD4+CD25+ regulatory T cell function by calcineurin dependent interleukin-2 production. *Blood* 2006;7:7.
9. Nakajima A, et al. Antigen-specific T cell-mediated gene therapy in collagen-induced arthritis. *J Clin Invest* 2001;107:1293–301. [PubMed: 11375419]
10. Tarner IH, et al. Retroviral gene therapy of collagen-induced arthritis by local delivery of IL-4. *Clin Immunol* 2002;105:304–14. [PubMed: 12498812]

11. Serrano LM, et al. Differentiation of naive cord-blood T cells into CD19-specific cytolytic effectors for posttransplantation adoptive immunotherapy. *Blood* 2006;107:2643–52. Epub 2005 Dec 13. [PubMed: 16352804]
12. Huang X, et al. Stable gene transfer and expression in human primary T cells by the Sleeping Beauty transposon system. *Blood* 2006;107:483–91. [PubMed: 16189271]
13. Kim YJ, Dubey P, Ray P, Gambhir SS, Witte ON. Multimodality imaging of lymphocytic migration using lentiviral-based transduction of a tri-fusion reporter gene. *Mol Imaging Biol* 2004;6:331–40. [PubMed: 15380743]
14. Tannous BA, Kim DE, Fernandez JL, Weissleder R, Breakefield XO. Codon-optimized Gaussia luciferase cDNA for mammalian gene expression in culture and in vivo. *Mol Ther* 2005;11:435–43. [PubMed: 15727940]
15. Riviere I, Brose K, Mulligan RC. Effects of retroviral vector design on expression of human adenosine deaminase in murine bone marrow transplant recipients engrafted with genetically modified cells. *Proc Natl Acad Sci U S A* 1995;92:6733–7. [PubMed: 7624312]
16. Brentjens RJ, et al. Eradication of systemic B-cell tumors by genetically targeted human T lymphocytes co-stimulated by CD80 and interleukin-15. *Nat Med* 2003;9:279–86. [PubMed: 12579196]
17. Brentjens RJ, et al. Genetically targeted T cells eradicate systemic acute lymphoblastic leukemia xenografts. *Clin Cancer Res* 2007;13:5426–35. [PubMed: 17855649]
18. Gong MC, et al. Cancer patient T cells genetically targeted to prostate-specific membrane antigen specifically lyse prostate cancer cells and release cytokines in response to prostate-specific membrane antigen. *Neoplasia* 1999;1:123–7. [PubMed: 10933046]
19. Costa GL, et al. Adoptive immunotherapy of experimental autoimmune encephalomyelitis via T cell delivery of the IL-12 p40 subunit. *J Immunol* 2001;167:2379–87. [PubMed: 11490028]
20. Gattinoni L, et al. Acquisition of full effector function in vitro paradoxically impairs the in vivo antitumor efficacy of adoptively transferred CD8+ T cells. *J Clin Invest* 2005;115:1616–26. [PubMed: 15931392]
21. Hinrichs CS, Gattinoni L, Restifo NP. Programming CD8+ T cells for effective immunotherapy. *Curr Opin Immunol* 2006;18:363–70. [PubMed: 16616471]
22. Klebanoff CA, et al. Central memory self/tumor-reactive CD8+ T cells confer superior antitumor immunity compared with effector memory T cells. *Proc Natl Acad Sci U S A* 2005;102:9571–6. [PubMed: 15980149]
23. Badr CE, Hewett JW, Breakefield XO, Tannous BA. A highly sensitive assay for monitoring the secretory pathway and ER stress. *PLoS ONE* 2007;2:e571. [PubMed: 17593970]
24. Cheng G, Davis RE. An improved and secreted luciferase reporter for schistosomes. *Mol Biochem Parasitol* 2007;155:167–71. [PubMed: 17681388]
25. Suzuki T, Usuda S, Ichinose H, Inouye S. Real-time bioluminescence imaging of a protein secretory pathway in living mammalian cells using Gaussia luciferase. *FEBS Lett* 2007;581:4551–6. [PubMed: 17825828]
26. Remy I, Michnick SW. A highly sensitive protein-protein interaction assay based on Gaussia luciferase. *Nat Methods* 2006;3:977–9. [PubMed: 17099704]
27. Venisnik KM, Olafsen T, Gambhir SS, Wu AM. Fusion of Gaussia luciferase to an engineered anti-carcinoembryonic antigen (CEA) antibody for in vivo optical imaging. *Mol Imaging Biol* 2007;9:267–77. [PubMed: 17577599]
28. Pichler A, Prior JL, Piwnicka-Worms D. Imaging reversal of multidrug resistance in living mice with bioluminescence: MDR1 P-glycoprotein transports coelenterazine. *Proc Natl Acad Sci U S A* 2004;101:1702–7. [PubMed: 14755051]
29. Kalikin LM, et al. In vivo visualization of metastatic prostate cancer and quantitation of disease progression in immunocompromised mice. *Cancer Biol Ther* 2003;2:656–60. [PubMed: 14688471]
30. Koehne G, et al. Serial in vivo imaging of the targeted migration of human HSV-TK-transduced antigen-specific lymphocytes. *Nat Biotechnol* 2003;21:405–13. Epub 2003 Mar 24. [PubMed: 12652311]
31. Billotey C, et al. T-cell homing to the pancreas in autoimmune mouse models of diabetes: in vivo MR imaging. *Radiology* 2005;236:579–87. Epub 2005 Jun 21. [PubMed: 15972338]

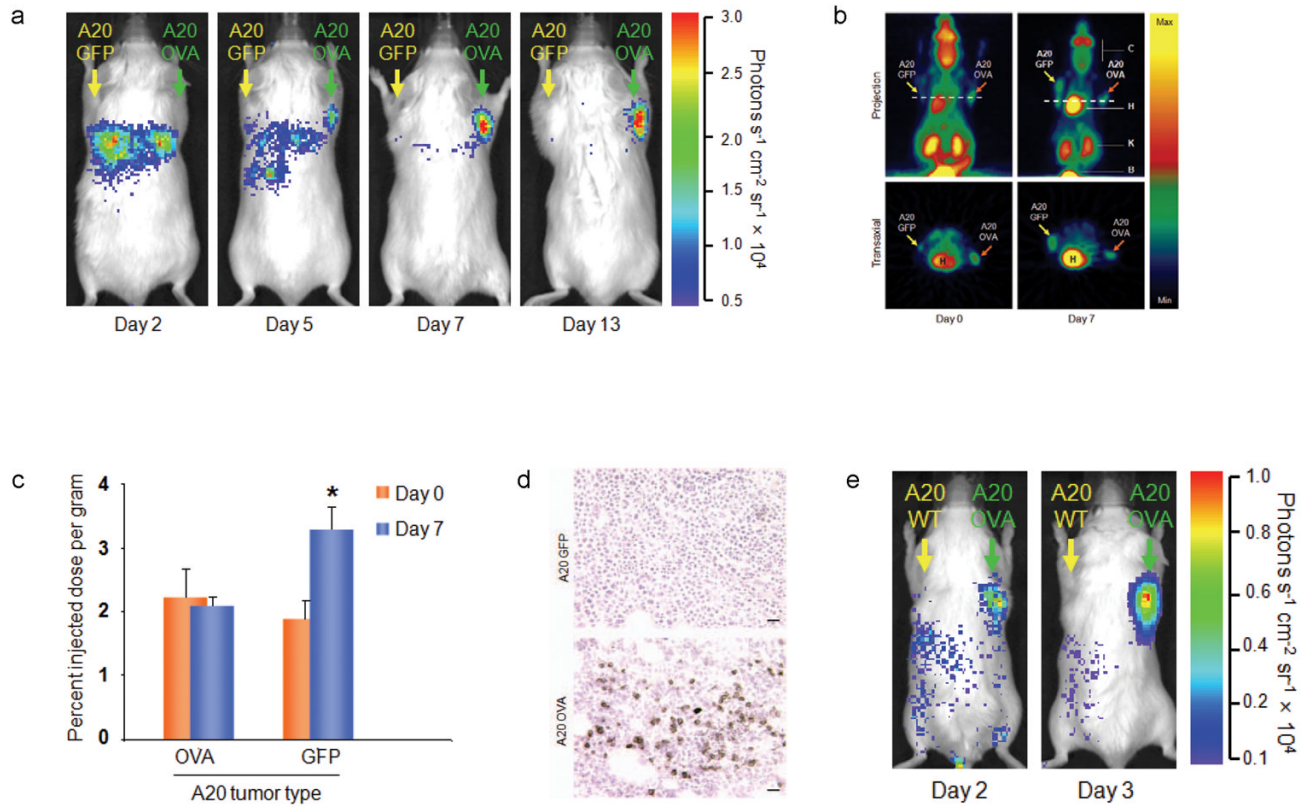
32. Hu DE, Kettunen MI, Brindle KM. Monitoring T-lymphocyte trafficking in tumors undergoing immune rejection. *Magn Reson Med* 2005;54:1473–9. [PubMed: 16276491]
33. Kircher MF, et al. In vivo high resolution three-dimensional imaging of antigen-specific cytotoxic T-lymphocyte trafficking to tumors. *Cancer Res* 2003;63:6838–46. [PubMed: 14583481]
34. Quintas-Cardama A, et al. Multifactorial optimization of gammaretroviral gene transfer into human T lymphocytes for clinical application. *Hum Gene Ther* 2007;18:1253–60. [PubMed: 18052719]
35. Latouche JB, Sadelain M. Induction of human cytotoxic T lymphocytes by artificial antigen-presenting cells. *Nat Biotechnol* 2000;18:405–9. [PubMed: 10748520]
36. Gade TP, et al. Targeted elimination of prostate cancer by genetically directed human T lymphocytes. *Cancer Res* 2005;65:9080–8. [PubMed: 16204083]

**Figure 1.**

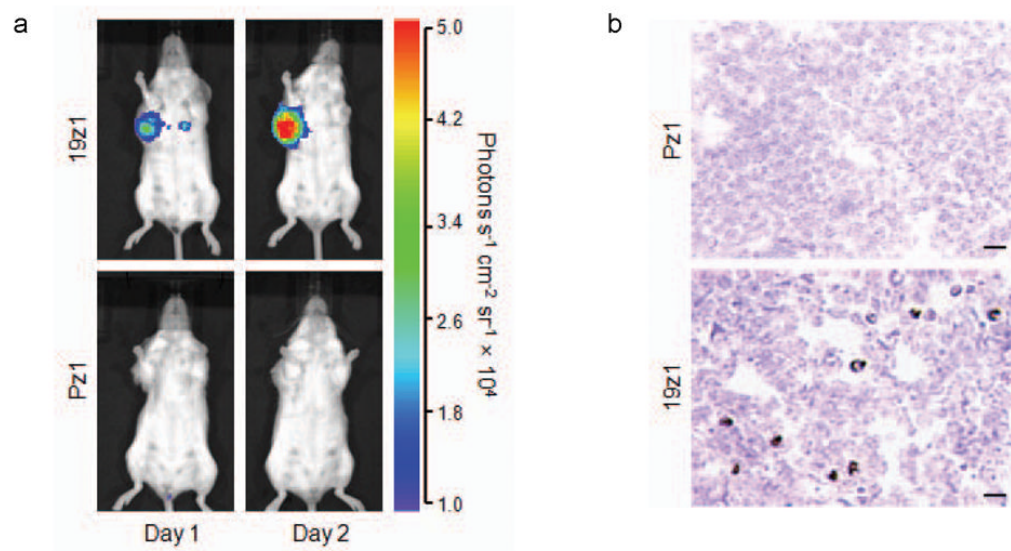
(a) Schematic representations of SFG luciferase constructs containing the native secreted GLuc, extGLuc, RLuc, extRLuc, and GFP-FFLuc. All constructs other than GFP-FFLuc contained an IRES-hrGFP reporter cassette to determine transduction efficiency. Black box, human CD8 leader sequence; LTR, long terminal repeat; SD, splice donor; SA, splice acceptor; CD8, CD8 transmembrane domain; arrows, start of transcription. (b) Bioluminescent imaging of PG-13 retroviral producer cells expressing the luciferase constructs at 24 h of culture and signal from tissue culture supernatants. (c) Quantitative analysis of signal from Fig 1b demonstrate a majority of the GLuc signal (98%) is contained in the culture medium. Supernatants from PG-13 cells containing the extGLuc, RLuc, and extRLuc demonstrate the percentage of signal in the filtered supernatant (27, 48, and 57% respectively). Marks indicate a statistically significant difference between individual groups compared to extGLuc total signal (\*) and extGLuc cells (●) with  $P < 0.01$ . (d) *In vitro* time course of bioluminescent signal generated by PG-13 T cells demonstrates a plateau signal for GLuc and extGLuc<sup>+</sup> PG-13 cells of 10 min following the addition of coelenterazine. (e) FACS analysis of human T cells either untransduced, transduced with GLucIRES-GFP, extGLucIRES-GFP, or extGLuc labeled with murine GLuc specific monoclonal antibody verifying expression of extGluc on the cell surface. (f) Cytosin immunohistochemistry of human T cells transduced to express either extGluc or native GLuc stained with murine GLuc specific monoclonal antibody confirms surface expression of extGLuc but not the GLuc.

**Figure 2.**

(a) SCID-Beige mice injected with MHC mismatched C57BL6 T cells expressing extGLucIRES-hrGFP, RLucIRES-hrGFP, or GLucIRES-hrGFP, were imaged by BLI on d 1, 2, 5, and 7 following bolus intravenous injection of coelenterazine. (b) Quantitative analysis of signal at each time point. Asterisk represents a significant difference ( $P < 0.001$ ) when RLuc or GLuc is compared to extGLuc. Data represents one of three experiments with similar results with five mice in each cohort. (c) *In vivo* time course characterization of bioluminescent signal comparing the extGLuc, RLuc and GLuc constructs was obtained on d 7 following allogeneic T cell infusion by obtaining 30 sec acquisitions per minute for 30 min. Once more, the extGLuc<sup>+</sup> T cell signal was >15 fold greater over 2–3 min following substrate infusion than that seen in mice infused with either RLuc<sup>+</sup> or GLuc<sup>+</sup> alloreactive C57BL6 T cells. (d) Presence of C57BL6 extGLuc T cells at sites commonly associated with GvHD, including the gut, skin (pinna), lung, liver, and spleen was confirmed by BLI. (e) Presence of T cells and the existence of graft versus host disease is evident in H&E tissue stains. Black arrows shown in the lung, liver, esophagus, and stomach photomicrographs demonstrate the presence of lymphocytes and histiocytes. Increased numbers of mitotic figures, as well as apoptotic and necrotic epithelial cells, are evident in the small intestine, stomach, and esophagus (red arrows). The spleen microsection shows highly mitotic T cells (black arrows) in the red pulp area not present in normal SCID-Beige mouse spleens (data not shown).

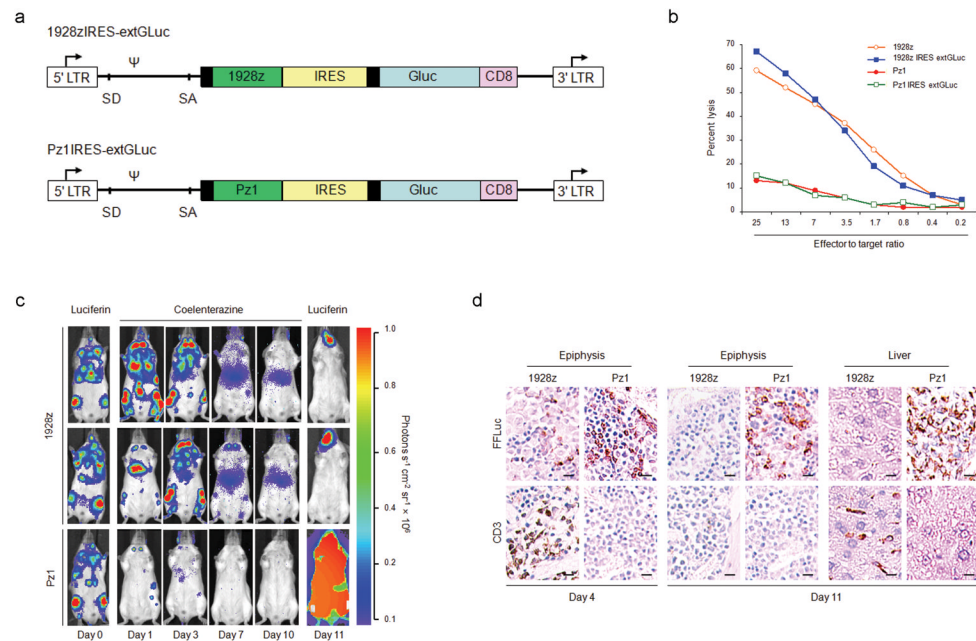
**Figure 3.**

(a) SCID-Beige mice bearing A20(OVA) and A20(GFP) subcutaneous tumors infused with extGLuc<sup>+</sup> DO11.10 OVA specific T cells were imaged by BLI over 13 days demonstrating initial T cell retention in the lung followed by increasing infiltration of T cells in the A20(OVA) tumor but not the A20(GFP) tumor over time. Data is representative two similar experiments with five treated mice in each experiment with similar results. (b) PET images visualizing A20 (OVA) and A20(GFP) tumors at d 0 show a larger A20(OVA) tumor when compared to A20 (GFP) tumor. By d 7, the A20(OVA) tumor appears decreased in size in contrast to the A20 (GFP) tumor which has progressed. (c) Quantitative signal of A20(GFP) and A20(OVA) tumor as assessed by PET demonstrates stable signal in the DO11.10 T cell infiltrated A20(OVA) tumor consistent with anti-tumor efficacy of infused T cells, while the A20(GFP) tumor demonstrates statistically significant progressive signal by PET consistent with unabated tumor growth (asterisk represents  $P < 0.01$ ). (d) Immunohistochemistry of A20(GFP) and A20(OVA) tumors at d 13 following adoptive therapy, demonstrating DO11.10 T cells infiltrating the A20 (OVA) tumor, with no evidence of T cell infiltration in A20(GFP) tumors. (e) Balb/c mice bearing subcutaneous A20(OVA) and wild type A20 tumors were injected by tail vein with extGLuc<sup>+</sup> DO11.10 OVA specific T cells, and monitored by BLI. At d 2 and 3, extGLuc<sup>+</sup> DO11.10 T cell infiltration is apparent in the A20(OVA) but not the wild type A20 tumor. Data represents one of five treated mice with similar results.



**Figure 4.**

(a) BLI of SCID-Beige mice bearing NALM-6 subcutaneous tumors following infusion of human 19z1<sup>+</sup>exGLuc<sup>+</sup> or Pz1<sup>+</sup>exGLuc<sup>+</sup> T cells. At 24 and 48 h following T cell injection, mice treated with 19z1<sup>+</sup>exGLuc<sup>+</sup> T cells demonstrated bioluminescent signal in the NALM-6 tumor, in contrast to mice treated with Pz1<sup>+</sup>exGLuc<sup>+</sup> T cells. Five mice were treated in each cohort with similar results. (b) Immunohistochemistry of tumor at 48 h demonstrates the presence of human CD8<sup>+</sup> T cells in 19z1<sup>+</sup>exGLuc<sup>+</sup> T cell treated mice, but not in Pz1<sup>+</sup>exGLuc<sup>+</sup> T cell treated mice, consistent with the bioluminescent images.

**Figure 5.**

**(a)** Bicistronic retroviral vectors 1928zIRES-extGLuc and Pz1IRES-extGLuc. Black box, human CD8 leader sequence; LTR, long terminal repeat; SD, splice donor; SA, splice acceptor; CD8, CD8 transmembrane domain; arrows, start of transcription. **(b)** 1928zIRES-extGLuc<sup>+</sup> T cells demonstrate similar cytotoxic potential when compared to 1928z<sup>+</sup> T cells as assessed by a standard 4 h <sup>51</sup>Cr release assay targeting NALM-6 tumor cells. Effector cell number represents the CD8<sup>+</sup> transduced T cell fraction. Assay was performed in triplicate wells with percent cytotoxicity varying <10% within each data set. Infused T cell populations in both treatment groups retained a central memory phenotype (CD62L<sup>hi</sup>CCR7<sup>+</sup>) (data not shown). **(c)** SCID-Beige mice bearing systemic NALM-6(GFP-FFLuc) tumor cells demonstrate diffuse tumor involvement by BLI on d 0. Following T cell infusion, T cells were imaged serially by BLI. 1928zIRES-extGLuc<sup>+</sup> T cell signal is noted at tumor sites in the bone marrow, liver, spleen and lymphnodes on d 1 and 3. Reduced signal is noted at these sites on d 7 and 10, likely due to tumor cell eradication as evidenced by tumor cell BLI at d 11. Persistent signal appreciated in the abdomen of 1928zIRES-extGLuc<sup>+</sup> T cell treated mice represents residual T cells in the liver. These data are consistent with the notion that the 1928z CAR specifically mediates T cell accumulation at sites of CD19<sup>+</sup> NALM-6 tumor. Data represents one of three experiments with similar results. **(d)** Immunohistochemistry of mouse tissues d 4 and d 11 following T cell infusion.